

# Low frequency signal detection via correlated Ramsey measurements

Santiago Oviedo-Casado<sup>\*,‡</sup>, Javier Prior<sup>‡,§</sup>, Javier Cerrillo<sup>‡,§</sup>

<sup>\*</sup>Racah Institute of Physics, The Hebrew University of Jerusalem, Jerusalem 91904, Givat Ram, Israel

<sup>‡</sup>Departamento de Física - CIOyN, Universidad de Murcia, Murcia E-30071, Spain

<sup>§</sup>Área de Física Aplicada, Universidad Politécnica de Cartagena, Cartagena E-30202, Spain

Dynamical decoupling protocols often rely on adjusting the time separation between pulses to match the half period of the target signal, limiting their scope to signals whose period is shorter than the characteristic decoherence time of the probe. We show that, in the low frequency regime, rather than struggling to fit dynamical decoupling sequences, it is more advantageous to perform Ramsey measurements carefully controlling the time at which each measurement is initiated. With such time-tagging, information about the phase of the signal is recorded, which crucially allows correlating measurements in post-processing, leading to efficient spectral reconstruction.

Identifying weak signals in the low frequency regime of the electromagnetic spectrum is paramount for the study of a wide variety of physical systems, ranging from low energy fundamental particles, such as neutrinos or axions [1], to chemical bonds (J-couplings) [2, 3], and material defects [4]. As a consequence, the last years have witnessed an effort to develop quantum sensors operating in this regime, which could be revolutionary for quantum information processing [5], quantum communications and radar applications [6, 7], biomedical imaging [8–10], nuclear quadrupole resonance [11, 12], or even alien life detection [13]. However, existing sensors based on, e.g., Rydberg atoms [14, 15], optomechanical sensors [16, 17], or superconducting circuits [18], are restricted by sophisticated setups and very low temperatures.

The typical quantum sensing setup features a carefully controlled quantum probe prepared on an initial coherent superposition state. Interaction with an external signal alters the quantum trajectory of the probe, making its final state dependent on a number of parameters  $\mathbf{a} = (a^1, a^2, \dots)$  describing the external signal, which is the underlying principle of quantum sensing. Repeating the measurement process to gather statistics allows to estimate the signal parameters contained in  $\mathbf{a}$ . Yet this very same measurement process means that the system interacts with a noisy environment that hinders the performance of the quantum sensor. Such noise causes two distinct processes, namely, dephasing or  $T_2^*$  noise, that describes the characteristic survival time of a coherent superposition state, and relaxation or  $T_1$  noise, which is the time the qubit takes to return to its equilibrium state [19]. Noise is thought to impose a fundamental constraint on the ability to detect signals whose frequency is smaller than the inverse characteristic dephasing time [20]. Here, we challenge this limitation.

During the evolution time, control sequences are applied to ensure sensitivity to the signal of interest, and to avoid interaction with unwanted noise. The Ramsey

sequence lets the probe evolve freely, making it most sensitive to the slowest frequency component of the noise spectrum, for which reason Ramsey spectroscopy is traditionally used to estimate parameters from static signals. In a Ramsey measurement, the probe is sensitive to all noise sources and, consequently, it is only useful if its interrogation time  $\tau_R$  is such that  $\tau_R < T_2^*$ . Detecting oscillating signals requires suppressing the sensitivity to the noisy frequencies lower than that of the target signal,  $\omega$ , achieved through a family of control sequences collectively known as dynamical decoupling (DD) [21–23]. They comprise pulses intended to refocus the probe and to filter out noise frequencies below  $\omega_{DD} = \pi/\tau$ , with  $\tau$  the pulses separation [22]. This has two consequences: on the one hand, DD demands  $\omega_{DD} \approx \omega$ , fixing upfront the duration of the corresponding sequence. On the other hand, DD extends the decoherence time of the qubit to  $T_2 \geq T_2^*$  [19, 24], which is typically determined experimentally [25]. Both facts together mean that the spacing between pulses in DD cannot exceed  $T_2$ , posing a problem for low frequency signals  $\omega < \pi/T_2$ , as DD sequences cannot eliminate the noise around the target signal's frequency. Moreover, even a DD extended  $T_2$  time is ultimately limited by  $T_2 < T_1$ , so that sensing sufficiently low frequencies is not possible with DD.

In this article, we propose the *correlated Ramsey* protocol for quantum parameter estimation of low frequency signals, which uses the quantum heterodyne (Qdyne) technique [26–28] to make the Ramsey sequence suitable for oscillating signals. Noting that the frequency matching requirement  $\omega_{DD} \approx \omega$  has no analogue in the case of the Ramsey sequence, such an experiment is appropriate for the detection of low frequencies, as opposed to an equivalent DD sequence, with the additional advantage of reducing the complexity of the experiment. The correlated Ramsey protocol is sensitive to the *coherent* phase of the target signal, making it distinguishable from *incoherent* noisy background signals of similar frequency, a feature which a DD sequence, being insensitive to the phase, cannot reproduce. Similar Ramsey-like synchronised measurements have been applied to the detection of high frequency signals [29, 30], for which purpose an artificial detuning that brings the frequency within

<sup>\*</sup>oviedo.cs@mail.huji.ac.il

<sup>‡</sup>javier.prior@um.es

<sup>§</sup>javier.cerrillo@upct.es

the sensor range is introduced through an external local oscillator that controls the sampling rate. Rather, we propose using the information about the target signal's phase that the Qdyne measurement protocol acquires, as the key which allows a Ramsey sequence to be maximally sensitive to oscillating signals. Our proposal overcomes the decoherence time limitation for low frequency signal detection for any quantum probe.

*Formal definitions* — Consider a qubit probe interacting with the longitudinal component of an external signal  $S(t, \mathbf{a})$ , that depends on some parameters  $\mathbf{a}$  and time [see Fig. 1(b)]. The interaction may be modeled by the Hamiltonian  $\sigma_z S(t, \mathbf{a})$ , with  $\sigma_z = |1\rangle\langle 1| - |0\rangle\langle 0|$ . The probe is additionally subject to transversal noise, which we treat through the Lindblad master equation formalism. Then, an initial superposition state on the probe experiences decoherence with a characteristic time  $T_s$  that depends on the environment of the qubit and on the control sequence ( $s$ ) used. For Ramsey,  $T_R = T_2^*$ , and  $T_{DD} = T_2$  for DD. The probability to find the qubit in its original state after some evolution time  $t$  is

$$P_s = \frac{1 + e^{-t/T_s} \cos [\Phi_s(t, \mathbf{a})]}{2}, \quad (1)$$

where  $\Phi_s(t, \mathbf{a})$  is the accumulated phase that depends on the specific sequence, the evolution time  $t$ , and the parameters in  $\mathbf{a}$  describing the external signal, which for the purpose of this article are the frequency  $a^1 = \omega$ , the amplitude  $a^2 = \xi$ , and the phase  $a^3 = \varphi$ .

We want to find the optimal control sequence that yields the smallest mean squared error  $\Delta a^k$  ( $k = 1, 2, \dots$ ) in the estimation of  $a^k$ , for a fixed experiment duration. According to the Cramér-Rao bound, the Fisher information ( $I_s^k$ ) contained on a sequence  $s$  about the parameter  $a^k$  bounds  $\Delta a^k$ , such that  $\Delta a^k \geq 1/I_s^k$  [31, 32]. We can then compare the performance of different sequences by computing their  $I_s^k$  with [33]

$$I_s^k = \frac{1}{P_s(1 - P_s)} \left( \frac{dP_s}{da^k} \right)^2, \quad (2)$$

which, considering Eq. (1), relates to  $\Phi_s$  through:

$$I_s^k = \frac{\sin^2 [\Phi_s(t, \mathbf{a})]}{\exp(2t/T_s) - \cos^2 [\Phi_s(t, \mathbf{a})]} \left[ \frac{d\Phi_s(t, \mathbf{a})}{da^k} \right]^2. \quad (3)$$

Repeated experiments additively increase the Fisher information, such that for  $N$  measurements spanning a total experiment time  $T$

$$I_{Ns}^k(T, \mathbf{a}_1) = \sum_{j=1}^N I_s^k(\tau_s, \mathbf{a}_j), \quad (4)$$

where we allow for modification of the external parameters for different experimental realizations  $\mathbf{a}_j$ .

We compare the performance of a single DD experiment featuring  $M$   $\pi$  pulses and of duration  $T = M\tau$ , with  $N$  Ramsey experiments of total equivalent duration

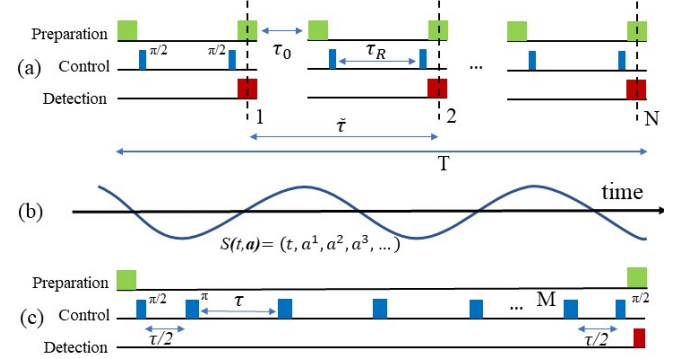


Figure 1. (a) Correlated Ramsey protocol composed of  $N$  Ramsey measurements repeated sequentially every  $\tilde{\tau}$ , which includes the measurement time  $\tau_R$  and an overhead time  $\tau_o$  for qubit readout and initialization, such that the total duration of the protocol is  $T = N\tilde{\tau}$ . (b) Low frequency target signal  $S(t, \mathbf{a})$ . (c) Dynamical decoupling sequence of equivalent duration  $T = M\tau$  featuring  $M$   $\pi$  pulses with even time separation  $\tau$ . For a low frequency, it becomes impossible to match the pulse separation in DD with the half period of the signal within the decoherence time of the probe, severely degrading the sensing ability.

$T = N\tilde{\tau}$ , where  $\tilde{\tau}$  is the sum of the duration of the experiment  $\tau_R$  and an overhead time  $\tau_o$ , as depicted in Fig. 1. To do so, we resort to the gain

$$g^k \equiv \frac{I_{NR}^k(T)}{I_{DD}^k(T)}. \quad (5)$$

In the limit of low frequencies we show that, for a wide range of parameters,  $g^k$  grows exponentially as the frequency of the external signal decreases, demonstrating that correlated Ramsey experiments beat sophisticated DD sequences for low frequency sensing.

*Single Ramsey experiment* — We begin by considering the Ramsey sequence, which consists on the free evolution of the qubit over a time  $\tau_R$ . The qubit is initially prepared on a superposition state  $\Psi(0) = (|0\rangle + |1\rangle)/\sqrt{2}$  by means of a  $\pi/2$  pulse. A final  $\pi/2$  pulse rotates the qubit back to the measurement basis. Note that all pulses will be considered here as having negligible duration (also known as the impulsive limit) and with amplitude much smaller than the energy gap of the qubit. During the free evolution time, the superposition accumulates a phase  $\Phi_R(t, \mathbf{a}) = \int_0^t dt' S(t', \mathbf{a})$  due to the external signal. Assuming that  $S(t, \mathbf{a}) = \xi \cos(\omega t + \varphi)$ , at the end of the sequence the total accumulated phase is

$$\Phi_R(\tau_R, \mathbf{a}) = \xi \tau_R \cos \left( \frac{\omega \tau_R}{2} + \varphi \right) \text{sinc} \left( \frac{\omega \tau_R}{2} \right). \quad (6)$$

Typically, sensitivity to external signals is quantified through the filter function (FF) of a given sequence, which corresponds to  $\langle \Phi_R(\tau_R, \mathbf{a})^2 \rangle_\varphi$ , the brackets denoting an average over the signal's phase. For Ramsey spectroscopy, the FF reads  $F_R(\omega) = \xi^2 \tau_R^2 \text{sinc}^2(\omega \tau_R/2)/2$  [34], which peaks at vanishing frequency, supporting the

idea that Ramsey sequences are mostly sensitive to static signals. Yet Eq. (6) indicates that this need not be the case if the phase of the signal is taken into account. For measurements performed at random initial times, information about  $\varphi$  is lost, and the relevant equation describing an experimental outcome is the FF. If the starting time  $t_j$  of each sequence is recorded, we can write  $\varphi_j = \omega t_j + \varphi$ , such that information about  $\varphi$  is conserved. A suitable measurement can then retrieve this information through the dependency in the phase expressed in Eq. (6) (see Appendix A for details).

*Dynamical decoupling* — DD sequences are constructed by embedding  $\pi$  pulses in between initialization and readout of the qubit. These pulses invert the state of the qubit with respect to a specific axis on the Bloch sphere. The effect of  $M$   $\pi$  pulses on the total accumulated phase can be computed by means of a response function  $h_M(t)$ , which has a unit absolute value, but changes sign every time a  $\pi$  pulse is applied. Then, the accumulated phase on the qubit is the convolution of  $h_M(t)$  and the external signal  $S(t, \mathbf{a})$  [34], yielding

$$\Phi_{DD}(T, \mathbf{a}) = -\xi\tau \cos\left(M\frac{\omega\tau + \pi}{2} + \varphi\right) \frac{\sin(M\frac{\omega\tau + \pi}{2})}{\cos(\frac{\omega\tau}{2})} \sin\left(\frac{\omega\tau}{4}\right) \text{sinc}\left(\frac{\omega\tau}{4}\right). \quad (7)$$

DD sequences create a filter around their characteristic frequency  $\omega_{DD} = \pi/\tau$ , whose width is inversely proportional to the number of pulses. Such a filter effect can be better understood studying the accumulated phase around the maximally sensitive region. Expanding Eq. (7) around  $\delta = \omega - \omega_{DD} \ll \omega$  the accumulated phase yields  $\Phi_{DD}(T, \mathbf{a}) \sim 2\Phi_R(T, \mathbf{a})/\pi$ , showing that DD is equivalent to a Ramsey sequence in which the qubit frame of reference rotates at similar angular frequency as the target signal.

*Fisher information* — All equations above are exact within the impulsive limit. In order to easily interpret the (also exact) numerical results ahead, we now derive an approximate expression for the low frequency limit of the gain  $g^k$ . In the low frequency limit, most terms resulting from the derivative in Eq. (3) vanish, and we keep only those proportional to the sinc function. In DD, when the experiment duration is  $T > T_2$ , the first term in Eq. (3) can be upper bound by  $\exp(-2T/T_2)$ , and we apply the same bound for correlated Ramsey. Note that, in correlated Ramsey, dephasing affects each measurement individually and not the global sequence, as the qubit is repolarized into its  $|0\rangle$  state after each measurement, which means that the exponential is a common upper bound of all terms in Eq. (4). Then, the sum in Eq. (4) can be simplified noting that the derivatives of oscillating functions can be written as phase-shifts in Eq. (6).

Considering these approximations for the low frequency regime, and keeping only the leading order in the total measurement time  $T$  (more details in Appendix C

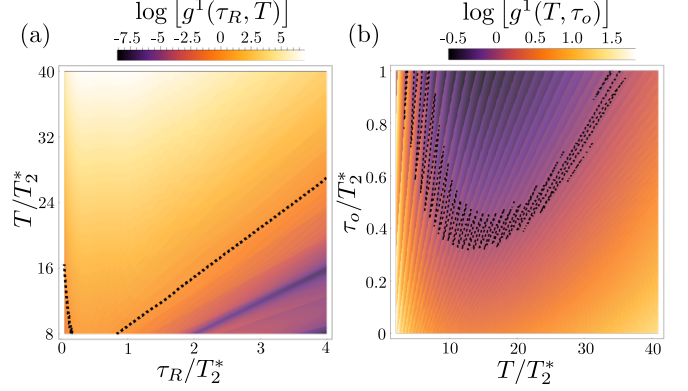


Figure 2. Logarithm of the exact gain  $g^1$  from Eq. (5). In (a),  $T_2 = 8T_2^*$  for a DD measurement of eight pulses, with  $\tilde{\tau} = 0.5T_2^* + \tau_R$  for correlated Ramsey. In (b),  $T_2 = 30T_2^*$  for a Hahn echo sequence, with  $T = 2\tau$  ranging from  $2T_2^*$  to  $40T_2^*$ . Here  $\tau_R = 0.5T_2^*$  such that  $\tilde{\tau} = 0.5T_2^* + \tau_o$ . In both figures the dashed line indicates the boundary  $g^1 = 1$ , we consider the amplitude  $\xi = 1/T_2^*$  to be the same in both protocols, and choose  $N$  for the Ramsey sequences such that  $N = \lfloor T/\tilde{\tau} \rfloor$ , the integer part of the quotient. Note that in both figures  $\omega = \pi/\tau$ .

and [26]), for correlated Ramsey

$$I_{NR}^k(T) = f_{NR}^k(T) \frac{\tau_R^2 T}{2\tilde{\tau}} e^{-2\tau_R/T_2^*}, \quad (8)$$

with  $f_s^k$  a factor that depends on the specific target parameter  $a^k$  and sequence  $s$  employed. Here  $f_{NR}^1 = \xi^2 T^2/3$ ,  $f_{NR}^2 = 1$ , and  $f_{NR}^3 = \xi^2$ .

For a single DD measurement

$$I_{DD}^k(T) = f_{DD}^k(T) \frac{T^2}{2\pi^2} e^{-2T/T_2}, \quad (9)$$

with  $f_{DD}^1 = 3f_{NR}^1$  and  $f_{DD}^2 = 4f_{NR}^2$ . Note that, since individual DD measurements are not sensitive to the phase,  $I_{DD}^3 = 0$ . Rather, Eq. (9) includes a phase averaging that decreases the total Fisher information by a factor of two.

*Exponential gain  $g^k$*  — Dividing Eq. (8) by Eq. (9) gives us

$$\lim_{\omega \rightarrow 0} g^k = e^{2\left(\frac{T}{T_2} - \frac{\tau_R}{T_2^*}\right)} \frac{\pi^2 \tau_R^2}{T \tilde{\tau}} f^k, \quad (10)$$

with  $f^1 = 1/3$  and  $f^2 = 1/4$ . Eq. (10) shows that  $g^k$  grows exponentially for frequencies  $\omega < \pi/T_2$  that require  $T > T_2$ . In this regime, we show that correlated Ramsey with a small  $\tau_R$  is preferred over DD. In Fig. 2 we use  $T_2^*$  as unit of measure, and calculate the gain  $g^1$  for the frequency *exactly*, using Eq. (5) with the accumulated phases Eqs. (6) and (7), assuming the frequency matching condition  $\omega = \pi/\tau$  for DD. The approximate expression Eq. (10), which reproduces well the trends observed in the exact results, as shown in Appendix D, can then be used to gain insight into the behaviour of each

protocol in the low frequency regime. The gain  $g^2$  for amplitude estimation has been shown to produce numerical results similar to  $g^1$ .

The probe coherence time is usually modelled as a function that grows sublinearly with the number of pulses  $M$  [25]. In Fig. 2(a) we favour DD considering that  $T_2 = MT_2^*$  (with  $M = 8$ ), and vary  $\tau_R$  aiming for detection of a signal with  $\omega < \pi/T_2$ . We observe that it is always possible to find a  $\tau_R$  such that correlated Ramsey proves superior whenever  $T > T_2$ . However, the question remains of what happens for slightly larger frequencies (such that the duration of the sequence  $T$  can fit within the coherence time  $T_2$ ), but which still remain small enough (such that  $T$  must be larger than the dephasing time  $T_2^*$ ). We provide an answer in Fig. 2(b), where we fix  $\tau_R$  to an optimal  $0.5T_2^*$  [from Fig. 2(a)],  $M = 1$  such that  $\tau = T/2$ , and take  $T_2 = 30T_2^*$ . We see that, as expected, correlated Ramsey benefits from a reduced overhead time  $\tau_o$  during which no information is acquired. From Fig. 2, we can conclude that, choosing adequate sequence parameters, correlated Ramsey outperforms DD for the detection of signals whose frequency is  $\omega < \pi/T_2$ , even for the stringent condition of a  $T_2$  that grows linearly with the number of pulses.

*Detection and sensitivity* — We now turn to the absolute values of Fisher information that can be achieved. In Fig. 3(a) we calculate the exact  $I_s^1$  of frequency estimation for a total measurement time  $T = 1000T_2^*$ , and compare it with the minimal amount of information –lying above the shadowed region– that is required for a successful parameter estimation, defined by the Rayleigh criterion (RC) of classical optics to be  $I_s^1 > 4/\omega^2 = 1/\Delta\omega_{RC}$  [35–37]. We calculate  $I_{NR}^1$  for two instances of the phase  $\varphi$  of the signal, and averaging out such phase. While particular phases cause oscillations of  $I_{NR}^1$  at low frequencies, an experiment which measures several time-traces with arbitrary phases on each of them [38] shall have no problem in estimating any arbitrarily low frequency, provided the measurement time  $T$  is sufficiently long. Contrary to that,  $I_{DD}^1$  decreases dramatically for low frequencies.

We also demonstrate the ability of the correlated Ramsey protocol to capture information about the phase of a low frequency signal. Fig. 3(b) shows the exact  $I_{NR}^3$  for phase estimation in two instances of a low frequency and two different durations  $T$ . We define the RC for the estimation of  $\varphi$  as having a MSE smaller than a 5% of the search interval  $\varphi \in [0, 2\pi]$ . Then,  $\Delta\varphi < \pi/10$  and a successful estimation requires  $I_{NR}^3 > 10/\pi$ . We can see that beating the resolution limit is simply a matter of increasing the measurement time.

Finally, in Fig. 3(c) we calculate the sensitivity to the frequency as a function of the total measurement time  $T$ , which following [19] can be defined as  $\eta_s = \sqrt{I_s^1/T}$ . We include two instances of  $T_2$  behaviour with DD  $\pi$  pulses, namely  $T_2 = MT_2^*$  and  $T_2 = M^{0.8}T_2^*$ . In both cases, the sensitivity of correlated Ramsey is far superior. Using DD for low frequency signals sensing could be useful only

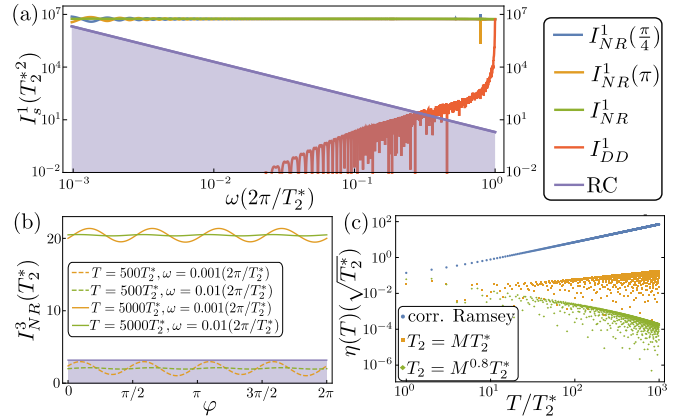


Figure 3. (a)  $I_{NR}^1$  for a correlated Ramsey sequence of duration  $T = 1000T_2^*$ , for two choices of  $\varphi$  and the phase-averaged result.  $I_{DD}^1$  for a DD sequence in which  $T_2 = MT_2^*$  and  $M = \lceil T\pi/\omega \rceil$ , the integer part of the quotient plus one, to ensure that, at least,  $M = 1$ . The shadowed area marks the region where  $I_s^1$  is not sufficient for frequency estimation, set here at  $\Delta\omega < \omega^2/4$  as per the Rayleigh criterion. (b)  $I_{NR}^3$  for two different frequencies  $\omega < \pi/T_2^*$  and  $T$ 's. Here, we impose a phase estimation criterion  $\Delta\varphi > \pi/10$ . (c) Sensitivity  $\sqrt{I_s^1/T}$  as a function of  $T$  for detection of a signal of frequency  $\omega = \pi/T_2^*$ , in correlated Ramsey and DD with  $T_2 = MT_2^*$  and  $T_2 = M^{0.8}T_2^*$ . Note that all  $I_s$ 's are calculated exactly and that  $\tau_R = \tau_o = 0.5T_2^*$  in all Figures, where we choose  $\xi = 1/\tau_R$  ( $\xi = 1/\tau$  for DD), which is optimal for parameter estimation [39]. Smaller values of  $\xi$  would just require larger  $T$ .

if the coherence time increases linearly with the number of pulses. Note however that even such an increase is limited, as  $T_2 \leq T_1$ . Consequently, for sufficiently low frequencies  $\omega < \pi/T_1$  DD can never beat the correlated Ramsey experiment that we introduce in this article

*Conclusions* — We propose the correlated Ramsey protocol for quantum sensing of low frequency signals. We demonstrate with exact numerical calculations that such a protocol outperforms DD sequences in the low frequency regime. We provide a simple but accurate analytical expression that permits estimating the adequate parameters to design tailored Ramsey sequences for any given target signal. Importantly, information about the phase of the signal can be acquired by performing sequential measurements with a precise time separation. This is the key that permits Ramsey measurements to become sensitive to oscillating signals, even though it is originally intended for static signals.

Signal processing for parameter estimation can be done through a variety of methods, including maximum likelihood estimation [38], or via least squares fitting to a signal's correlation model or Fourier transform [39, 40]. The low frequency regime has thus far hardly been contemplated by quantum sensing protocols due to the difficulty of accessing it, despite it being crucial in the study of, for example, J coupling in molecules. Our proposal, whose simplicity with respect to complicated dynamical

decoupling sequences makes it all the more compelling, is an essential step forward in exploring this regime.

*Acknowledgements* — S.O.C. acknowledges the support from the *Fundación Ramón Areces* postdoctoral fellowship (XXXI edition of grants for Postgraduate Studies in Life and Matter Sciences in Foreign Universities and Research centers) as well as the Israeli Science Foundation and the ERC grant QRES, project number 770929. J.C. acknowledges support from *Ministerio de Ciencia, Innovación y Universi-*

*dades* (Spain) (“Beatrix Galindo” Fellowship BEAGAL18/00078). J.P. acknowledges support from the QuantERA II Programme (Mf-QDS) that has received funding from the European Union’s Horizon 2020 research and innovation programme under Grant Agreement No 101017733, Grant Agreement No. PCI2022-132915 MCIN/AEI/10.13039/501100011033 and European Union “NextGenerationEU”/PRTR” and Grant Agreement No. PID2021-124965NB-C21 MCIN/AEI/10.13039/501100011033/ and by FEDER “A way to make Europe”.

---

[1] ECFA Detector R&D Roadmap Process Group, *The 2021 ECFA detector research and development roadmap*, Tech. Rep. (Geneva, 2020).

[2] A. Soncini and P. Lazzaretti, “Nuclear spin-spin coupling density in molecules,” *The Journal of Chemical Physics* **118**, 7165–7173 (2003).

[3] Kiplangat Sutter and Jochen Autschbach, “Computational study and molecular orbital analysis of nmr shielding, spin–spin coupling, and electric field gradients of azido platinum complexes,” *Journal of the American Chemical Society* **134**, 13374–13385 (2012).

[4] P. Bevington, R. Gartman, and W. Chalupczak, “Enhanced material defect imaging with a radio-frequency atomic magnetometer,” *Journal of Applied Physics* **125**, 094503 (2019).

[5] Sridhar Majety, Pranta Saha, Victoria A. Norman, and Marina Radulaski, “Quantum information processing with integrated silicon carbide photonics,” *Journal of Applied Physics* **131**, 130901 (2022).

[6] V. Gerginov, F. C. S. da Silva, and D. Howe, “Prospects for magnetic field communications and location using quantum sensors,” *Review of Scientific Instruments* **88**, 125005 (2017).

[7] Quntao Zhuang and Jeffrey H. Shapiro, “Ultimate accuracy limit of quantum pulse-compression ranging,” *Phys. Rev. Lett.* **128**, 010501 (2022).

[8] H. Xia, A. Ben-Amar Baranga, D. Hoffman, and M. V. Romalis, “Magnetoencephalography with an atomic magnetometer,” *Applied Physics Letters* **89**, 211104 (2006).

[9] J. Belfi, G. Bevilacqua, V. Biancalana, S. Cartaleva, Y. Dancheva, and L. Moi, “Cesium coherent population trapping magnetometer for cardiosignal detection in an unshielded environment,” *J. Opt. Soc. Am. B* **24**, 2357–2362 (2007).

[10] Kiwoong Kim, Samo Begus, Hui Xia, Seung-Kyun Lee, Vojko Jazbinsek, Zvonko Trontelj, and Michael V. Romalis, “Multi-channel atomic magnetometer for magnetoencephalography: A configuration study,” *NeuroImage* **89**, 143–151 (2014).

[11] A.N. Garroway, M.L. Buess, J.B. Miller, B.H. Suits, A.D. Hibbs, G.A. Barrall, R. Matthews, and L.J. Burnett, “Remote sensing by nuclear quadrupole resonance,” *IEEE Transactions on Geoscience and Remote Sensing* **39**, 1108–1118 (2001).

[12] S.-K. Lee, K. L. Sauer, S. J. Seltzer, O. Alem, and M. V. Romalis, “Subfemtotesla radio-frequency atomic magnetometer for detection of nuclear quadrupole resonance,” *Applied Physics Letters* **89**, 214106 (2006).

[13] Andrew P. V. Siemion, Paul Demorest, Eric Korpela, Ron J. Maddalena, Dan Werthimer, Jeff Cobb, Andrew W. Howard, Glen Langston, Matt Lebofsky, Geoffrey W. Marcy, and Jill Tarter, “A 1.1-1.9 GHz SETI SURVEY OF THE KEPLER FIELD. I.A SEARCH FOR NARROW-BAND EMISSION FROM SELECT TARGETS,” *The Astrophysical Journal* **767**, 94 (2013).

[14] Joshua A. Gordon, Christopher L. Holloway, Andrew Schwarzkopf, Dave A. Anderson, Stephanie Miller, Nithiwadee Thaicharoen, and Georg Raithel, “Millimeter wave detection via autler-townes splitting in rubidium rydberg atoms,” *Applied Physics Letters* **105**, 024104 (2014).

[15] David H. Meyer, Kevin C. Cox, Fredrik K. Fatemi, and Paul D. Kunz, “Digital communication with rydberg atoms and amplitude-modulated microwave fields,” *Applied Physics Letters* **112**, 211108 (2018).

[16] T. Bagci, A. Simonsen, S. Schmid, L. G. Villanueva, E. Zeuthen, J. Appel, J. M. Taylor, A. Sørensen, K. Usami, A. Schliesser, and E. S. Polzik, “Optical detection of radio waves through a nanomechanical transducer,” *Nature* **507**, 81–85 (2014).

[17] M.J. Rudd, P.H. Kim, C.A. Potts, C. Doolin, H. Ramp, B.D. Hauer, and J.P. Davis, “Coherent magneto-optomechanical signal transduction and long-distance phase-shift keying,” *Phys. Rev. Applied* **12**, 034042 (2019).

[18] Mario F. Gely, Marios Kounalakis, Christian Dickel, Jacob Dalle, Rémy Vatré, Brian Baker, Mark D. Jenkins, and Gary A. Steele, “Observation and stabilization of photonic fock states in a hot radio-frequency resonator,” *Science* **363**, 1072–1075 (2019).

[19] John F. Barry, Jennifer M. Schloss, Erik Bauch, Matthew J. Turner, Connor A. Hart, Linh M. Pham, and Ronald L. Walsworth, “Sensitivity optimization for nv-diamond magnetometry,” *Rev. Mod. Phys.* **92**, 015004 (2020).

[20] T. Joas, A. M. Waeber, G. Braunbeck, and F. Reinhard, “Quantum sensing of weak radio-frequency signals by pulsed mollow absorption spectroscopy,” *Nature Communications* **8**, 964 (2017).

[21] Lorenza Viola, Emanuel Knill, and Seth Lloyd, “Dynamical decoupling of open quantum systems,” *Phys. Rev. Lett.* **82**, 2417–2421 (1999).

[22] Lukasz Cywiński, Roman M. Lutchyn, Cody P. Nave,

and S. Das Sarma, “How to enhance dephasing time in superconducting qubits,” *Phys. Rev. B* **77**, 174509 (2008).

[23] C. L. Degen, M. Poggio, H. J. Mamin, and D. Rugar, “Role of spin noise in the detection of nanoscale ensembles of nuclear spins,” *Phys. Rev. Lett.* **99**, 250601 (2007).

[24] L. M. Pham, N. Bar-Gill, C. Belthangady, D. Le Sage, P. Cappellaro, M. D. Lukin, A. Yacoby, and R. L. Walsworth, “Enhanced solid-state multispin metrology using dynamical decoupling,” *Phys. Rev. B* **86**, 045214 (2012).

[25] G. de Lange, Z. H. Wang, D. Ristè, V. V. Dobrovitski, and R. Hanson, “Universal dynamical decoupling of a single solid-state spin from a spin bath,” *Science* **330**, 60–63 (2010).

[26] Simon Schmitt, Tuvia Gefen, Felix M. Stürner, Thomas Uden, Gerhard Wolff, Christoph Müller, Jochen Scheuer, Boris Naydenov, Matthew Markham, Sébastien Pezzagna, Jan Meijer, Ilai Schwarz, Martin Plenio, Alex Retzker, Liam P. McGuinness, and Fedor Jelezko, “Submillihertz magnetic spectroscopy performed with a nanoscale quantum sensor,” *Science* **356**, 832–837 (2017).

[27] J. M. Boss, K. S. Cujia, J. Zopes, and C. L. Degen, “Quantum sensing with arbitrary frequency resolution,” *Science* **356**, 837–840 (2017).

[28] David R. Glenn, Dominik B. Bucher, Junghyun Lee, Mikhail D. Lukin, Hongkun Park, and Ronald L. Walsworth, “High-resolution magnetic resonance spectroscopy using a solid-state spin sensor,” *Nature* **555**, 351–354 (2018).

[29] Jonas Meinel, Vadim Vorobyov, Boris Yavkin, Durga Dasari, Hitoshi Sumiya, Shinobu Onoda, Junichi Isoya, and Jörg Wrachtrup, “Heterodyne sensing of microwaves with a quantum sensor,” *Nature Communications* **12**, 2737 (2021).

[30] Nicolas Staudenmaier, Simon Schmitt, Liam P. McGuinness, and Fedor Jelezko, “Phase-sensitive quantum spectroscopy with high-frequency resolution,” *Phys. Rev. A* **104**, L020602 (2021).

[31] W. K. Wootters, “Statistical distance and hilbert space,” *Phys. Rev. D* **23**, 357–362 (1981).

[32] Samuel L. Braunstein and Carlton M. Caves, “Statistical distance and the geometry of quantum states,” *Phys. Rev. Lett.* **72**, 3439–3443 (1994).

[33] Tuvia Gefen, Fedor Jelezko, and Alex Retzker, “Control methods for improved fisher information with quantum sensing,” *Phys. Rev. A* **96**, 032310 (2017).

[34] J. Cerrillo, S. Oviedo Casado, and J. Prior, “Low field nano-nmr via three-level system control,” *Phys. Rev. Lett.* **126**, 220402 (2021).

[35] E. Abbe, “Beiträge zur theorie des mikroskops und der mikroskopischen wahrnehmung,” *Archiv für Mikroskopische Anatomie* **9**, 413–468 (1873).

[36] F.R.S. Lord Rayleigh, “XXXI. investigations in optics, with special reference to the spectroscope,” *The London, Edinburgh, and Dublin Philosophical Magazine and Journal of Science* **8**, 261–274 (1879).

[37] Bland-Hawthorn J. Jones A. W., Shopbell P., *Towards a General Definition for Spectroscopic Resolution*, edited by Hayes J. J. E. Shaw R. A., Payne H. E., Vol. 77 (Astronomical Society of the Pacific Conference Series, 1995) pp. 503–506.

[38] Amit Rotem, Tuvia Gefen, Santiago Oviedo-Casado, Javier Prior, Simon Schmitt, Yoram Burak, Liam McGuinness, Fedor Jelezko, and Alex Retzker, “Limits on spectral resolution measurements by quantum probes,” *Phys. Rev. Lett.* **122**, 060503 (2019).

[39] Santiago Oviedo-Casado, Amit Rotem, Ramil Nigmatullin, Javier Prior, and Alex Retzker, “Correlated noise in brownian motion allows for super resolution,” *Scientific Reports* **10**, 19691 (2020).

[40] Nicolas Staudenmaier, Anjusha Vijayakumar-Sreeja, Santiago Oviedo-Casado, Genko Genov, Daniel Cohen, Daniel Dulog, Thomas Uden, Nico Striegler, Alastair Marshall, Jochen Scheuer, Christoph Findler, Johannes Lang, Ilai Schwarz, Philipp Neumann, Alex Retzker, and Fedor Jelezko, “Power-law scaling of correlations in statistically polarised nano-nmr,” (2022), 10.48550/ARXIV.2203.11161.

## Appendix A: Accumulated phase

Let us begin by calculating the phase that a qubit superposition state accumulates when it is interacting with an external signal, and subject to either the Ramsey sequence or a generic dynamical decoupling sequence. Both sequences feature an initial  $\pi/2$  pulse that creates the superposition state on the qubit,  $\Psi(0) = (|0\rangle + |1\rangle)/\sqrt{2}$ , and a final  $\pi/2$  pulse after the evolution time which rotates the evolved state onto the measurement basis. Throughout, we consider that the pulses intended to control the qubit have negligible duration (impulsive limit), and that their amplitude is much smaller than the qubit energy gap.

### 1. Single Ramsey experiment

During the free evolution time  $\tau_R$  in the Ramsey sequence, the quantum probe superposition state evolves influenced by the external signal  $S(t, \mathbf{a})$  –where  $\mathbf{a} = (a^1, a^2, \dots)$  represents a vector of parameters describing said signal– such that after some time  $t$  the state of the probe is  $\Psi(t) = (|0\rangle + \exp[i\Phi_R(t, \mathbf{a})] |1\rangle)/\sqrt{2}$ , with  $\Phi_R(t, \mathbf{a})$  a phase that the probe accumulates, and which upon transformation onto the measurement basis and interrogation of the qubit state, reveals itself as a population difference between the states  $|0\rangle$  and  $|1\rangle$ . It is this population difference what carries the information about the external signal parameters  $\mathbf{a}$ .

For our purposes here, we consider a pure tone signal of cosine form, such that  $S(t, \mathbf{a}) = \xi \cos(\omega t + \varphi)$ , with

parameters  $a^1 = \omega$ ,  $a^2 = \xi$  and  $a^3 = \varphi$ . Then, for a Ramsey measurement starting at  $t = 0$  and with duration  $\tau_R$ , the accumulated phase is calculated as

$$\Phi_R(\tau_R, \mathbf{a}) = \xi \int_0^{\tau_R} dt \cos(\omega t + \varphi) = \xi \tau_R \cos\left(\frac{\omega \tau_R}{2} + \varphi\right) \text{sinc}\left(\frac{\omega \tau_R}{2}\right). \quad (\text{A1})$$

The accumulated phase Eq. (A1) can be rewritten as  $\xi \Re\{e^{i\varphi} F[h_R(t)]\}$ , the real part of the Fourier transform (or, alternatively, the cosine Fourier transform) of a function  $h_R(t) = 1$  in  $0 \leq t \leq \tau_R$  and zero otherwise. Such a function is called *response function*, and can be said to characterize the value of the coherence of the qubit probe during the evolution time. Describing the accumulated phase in terms of the Fourier transform of response functions proves useful for more complicated measurement sequences, as will be shown in the next subsection for dynamical decoupling.

To demonstrate that it is sensitivity to the phase of the external signal  $\varphi$  what allows Ramsey measurements to detect oscillating signals, we can solve Eq. (A1) analytically to find its maximum in the frequency  $\omega$ . This yields

$$\omega \tau_R = \tan(\omega \tau_R + \varphi) - \frac{\sin \varphi}{\cos(\omega \tau_R + \varphi)}. \quad (\text{A2})$$

For  $\varphi \neq n\pi$  the maximum phase accumulation occurs at a frequency  $\omega \neq 0$ .

The connection with usual experiments, in which the Ramsey sequence is mostly sensitive to static signals, can be made by squaring Eq. (A1), and averaging it with respect to the phase to get the filter function, which is the typical figure of merit for signal detection. Then

$$\langle \Phi_R(\tau_R, \mathbf{a})^2 \rangle_\varphi = \xi^2 \tau_R^2 \text{sinc}^2\left(\frac{\omega \tau_R}{2}\right) \frac{1}{2\pi} \int_0^{2\pi} d\varphi \cos^2\left(\frac{\omega \tau_R}{2} + \varphi\right) = \frac{\xi^2 \tau_R^2}{2} \text{sinc}^2\left(\frac{\omega \tau_R}{2}\right), \quad (\text{A3})$$

whose maximum occurs at  $\omega = 0$ .

## 2. Dynamical decoupling

Dynamical decoupling sequences are based on the Hahn echo of classical nuclear magnetic resonance [22]. As such, they comprise a number  $M$  of  $\pi$  pulses acting on the qubit probe during the evolution time, i.e. in between the two  $\pi/2$  pulses that initiate and end the measurement sequence. These  $\pi$  pulses are usually evenly spaced in time, with time separation  $\tau$ , and their intention is to rephase the qubit state. Specifically, when acting on the state  $\Psi(t, \mathbf{a})$ , they will invert the state with respect to a particular axis of the Bloch sphere.

To calculate the phase accumulated during a dynamical decoupling sequence, we again have to integrate the external signal for the duration of the evolution time, which for  $M \pi$  pulses applied is  $M\tau$ , where we consider that the separation between the first  $\pi$  pulse and the initial  $\pi/2$  pulse is  $\tau/2$  (see Fig. 1 on the main text for a depiction of both protocols). The same happens for the last  $\pi$  pulse and the  $\pi/2$  that finishes the sequence. Moreover, we have to consider the specific effect that each of the  $\pi$  pulses has on the qubit. To do so, we resort to the response function, and start off from the Ramsey sequence case, which is also valid to describe the value of the qubit coherence during a free evolution time  $\tau$ . Then, since  $\pi$  pulses reverse the sign of the qubit coherence, a dynamical decoupling sequence can be constructed using response functions of absolute value 1 and that change sign every time a  $\pi$  pulse is applied. For example, the case of a Hahn echo of duration  $\tau$ , with a  $\pi$  pulse applied at a time  $\tau/2$  is described as  $h_1(t) = h_R(t) - h_R(t - \tau/2)$ , where we have taken  $\tau_R = \tau/2$ . The generic dynamical decoupling sequence response function is constructed repeating the Hahn echo sequence every  $\tau$ , such that  $h_M(t) = \sum_{j=0}^{M-1} (-1)^j h_1(t - j\tau)$ . It is in this situation where writing the accumulated phase as a Fourier transform proves useful, as we can then apply the time shift property of the Fourier transform, that reads  $\mathcal{F}[h(t - t')] = \exp(i\omega t') \mathcal{F}[h(t)]$ , to the Ramsey sequence results, and calculate the accumulated phase on a generic dynamical decoupling sequence [34]. Beginning with the Hahn echo sequence and generalizing we get

$$\Phi_{DD}(T, \mathbf{a}) = -\xi \tau \cos\left(M \frac{\omega \tau + \pi}{2} + \varphi\right) \frac{\sin(M \frac{\omega \tau + \pi}{2})}{\cos(\frac{\omega \tau}{2})} \sin\left(\frac{\omega \tau}{4}\right) \text{sinc}\left(\frac{\omega \tau}{4}\right). \quad (\text{A4})$$

## Appendix B: Small detuning $\delta$ limit for dynamical decoupling

In this section, we calculate explicitly the small detuning limit  $\delta \rightarrow 0$  of the accumulated phase  $\Phi_{DD}(T, \mathbf{a})$  in a dynamical decoupling sequence with  $\omega_{DD} \approx \omega$ . Consider the full expression for  $\Phi_{DD}(T, \mathbf{a})$  in Eq. (A4). If the frequency

matching condition is met, such that  $\tau$  is chosen to satisfy  $\pi/\tau = \omega_{DD} \approx \omega$ , as it is generally required for a successful signal detection with dynamical decoupling sequences, we can write  $\omega_{DD} = \omega - \delta$ , with  $\delta \ll \omega$  a small detuning frequency. Then, using  $\omega_{DD} = \pi/\tau$ , the following holds:  $\omega\tau = \omega\pi/(\omega - \delta) = \pi/(1 - \delta/\omega) \approx \pi + \pi\delta/\omega + O(\delta^2) \approx \pi + \delta\tau$ , where in the last two steps we have made use of the small detuning assumption. A similar reasoning shows that  $M\omega\tau \approx M(\pi + \delta\tau)$ . Considering the terms which do not depend on  $M$  in Eq. (A4), we can write them as

$$\frac{4}{\omega\tau} \frac{\sin^2 \frac{\omega\tau}{4}}{\cos \frac{\omega\tau}{2}} = \frac{2}{\omega\tau} \frac{1 - \cos \frac{\omega\tau}{2}}{\cos \frac{\omega\tau}{2}} \approx \frac{2}{\omega\tau} \frac{1 - \cos \frac{\pi}{2(1 - \frac{\delta}{\omega})}}{\cos \frac{\pi}{2(1 - \frac{\delta}{\omega})}} \approx \frac{2}{\omega\tau} \frac{1 + \frac{\pi\delta}{2\omega} + O(\delta^2)}{-\frac{\pi\delta}{2\omega} + O(\delta^2)} \approx -\frac{4}{\pi\delta\tau}, \quad (\text{B1})$$

where the last steps involve a Taylor expansion around  $\delta = 0$ , keeping only the leading order in  $\delta$ . The terms that contain  $M$  are rewritten as

$$-\cos \left( M \frac{\omega\tau + \pi}{2} + \varphi \right) \sin \left( M \frac{\omega\tau + \pi}{2} \right) \approx -\cos \left( \frac{M\delta\tau}{2} + \varphi \right) \sin \left( \frac{M\delta\tau}{2} \right). \quad (\text{B2})$$

Bringing all together with a bit of trigonometry gives us that the following expression for the accumulated phase as a function of the detuning  $\delta$ :

$$\Phi_{DD}^\delta(T, \mathbf{a}) = \frac{2M\xi\tau}{\pi} \cos \left( \frac{M\delta\tau}{2} + \varphi \right) \operatorname{sinc} \left( \frac{M\delta\tau}{2} \right), \quad (\text{B3})$$

which coincides (up to a  $2/\pi$  factor) with Eq. (A1) by replacing the sequence duration  $M\tau \rightarrow \tau_R$  and  $\delta \rightarrow \omega$ .

### Appendix C: Detailed Fisher information calculations

We now provide a step by step derivation of the total Fisher information formulas, for a correlated Ramsey protocol and a dynamical decoupling sequence of equivalent total duration, in the low frequency limit, with which the approximate gain is calculated on the main text. We start from the expression for the Fisher information for a single instance of a general measurement sequence  $s$

$$I_s^k = \frac{\sin^2 [\Phi_s(t, \mathbf{a})]}{\exp(2t/T_s) - \cos^2 [\Phi_s(t, \mathbf{a})]} \left[ \frac{d\Phi_s(t, \mathbf{a})}{da^k} \right]^2, \quad (\text{C1})$$

with  $\Phi_s(t, \mathbf{a})$  the accumulated phase during that sequence. Focusing on the first factor, we can see that it oscillates between zero and  $\exp(-2t/T_s)$ . We want to compare the information accumulated due to Ramsey measurements with that accumulated by a dynamical decoupling sequence. For long measurement time  $T$  as required by dynamical decoupling sequences intended for low frequency signals, we can upper bound this first factor by  $\exp(-2T/T_2)$ , and we do the same for correlated Ramsey sequences, thus, the following approximate expressions for  $I_s^k$  represent upper bounds on the Fisher information. Additionally, we note that, in the low frequency limit, with  $\omega \rightarrow 0$ ,  $\operatorname{sinc}(\omega\tau/2) \rightarrow 1$ , while for the same reason the derivative  $\operatorname{sinc}'(\omega\tau/2) \rightarrow 0$ , therefore, we can safely neglect the terms including  $\operatorname{sinc}'(\omega\tau/2)$  in the calculation. This works for a Ramsey measurement. In the case of a dynamical decoupling sequence, the argument is the same but for the approximate formula Eq. (B3), in which, when the frequency matching condition of dynamical decoupling sequences is met,  $\delta \rightarrow 0$ .

We begin by calculating the Fisher information of correlated Ramsey. For an arbitrary Ramsey sequence we have that

$$I_R^k(\tau_R) = \exp(-2\tau_R/T_2^*) \left[ \frac{d\Phi_R(\tau_R, \mathbf{a})}{da^k} \right]^2. \quad (\text{C2})$$

The total Fisher information in a sequence of  $N$  measurements is obtained by summing the individual contributions from each Ramsey measurement composing the sequence. Notice that on implementing the correlated Ramsey protocol, we have to consider that at the end of each measurement the qubit is repolarized into its  $|0\rangle$  state, and consequently the dephasing affects each measurement individually. This means that on performing the sum of Fisher informations we can take the exponential term out of the summation, such that

$$I_{NR}^k(T) = \exp(-2\tau_R/T_2^*) \sum_{j=1}^N \left[ \frac{d\Phi_R(t_j, \mathbf{a})}{da^k} \right]^2. \quad (\text{C3})$$

Here,  $t_j$  defines the starting times of each Ramsey sequence in the protocol, with  $j$  running from 1 to  $N$ , and where the separation between consecutive measurements is such that  $t_{j+1} = t_j + \tilde{\tau}$ , with  $\tilde{\tau} = \tau_R + \tau_o$  including the overhead time  $\tau_o$  spent on interrogating the qubit probe at the end of each sequence, and reinitializing it for the next measurement. Considering a  $t_j$  starting time modifies Eq. (A1) adding an extra  $\omega t_j$  to the initial phase  $\varphi$ .

We begin with the case of the amplitude  $a^2 = \xi$ , and we consider  $t_1 = 0$  such that  $t_j = j\tilde{\tau}$ . Then, using  $N = T/\tilde{\tau}$ , we get that:

$$\sum_{j=1}^N \left[ \frac{d\Phi_R(\tau_R, \mathbf{a})}{d\xi} \right]^2 = \tau_R^2 \operatorname{sinc}^2 \left( \frac{\omega\tau_R}{2} \right) \sum_{j=1}^N \cos^2 \left( \omega t_j + \frac{\omega\tau_R}{2} + \varphi \right) \approx \frac{\tau_R^2 T \cos^2 \varphi}{\tilde{\tau}}, \quad (\text{C4})$$

where we have applied the low frequency limit  $\omega \rightarrow 0$ .

The case of the phase  $a^3 = \varphi$  is similar, yielding

$$\sum_{j=1}^N \left[ \frac{d\Phi_R(\tau_R, \mathbf{a})}{d\varphi} \right]^2 = \xi^2 \tau_R^2 \operatorname{sinc}^2 \left( \frac{\omega\tau_R}{2} \right) \sum_{j=1}^N \sin^2 \left( \omega t_j + \frac{\omega\tau_R}{2} + \varphi \right) \approx \frac{\xi^2 \tau_R^2 T \sin^2 \varphi}{\tilde{\tau}}. \quad (\text{C5})$$

The frequency  $a^1 = \omega$  contains a few more terms, but can be calculated in the same way:

$$\sum_{j=1}^N \left[ \frac{d\Phi_R(\tau_R, \mathbf{a})}{d\omega} \right]^2 = \tau_R^2 \xi^2 \operatorname{sinc}^2 \left( \frac{\omega\tau_R}{2} \right) \sum_{j=1}^N (t_j + \tau_R/2)^2 \sin^2 \left( \omega t_j + \frac{\omega\tau_R}{2} + \varphi \right) \quad (\text{C6})$$

$$= \tau_R^2 \xi^2 \operatorname{sinc}^2 \left( \frac{\omega\tau_R}{2} \right) \sum_{j=1}^N \left( t_j^2 + \frac{\tau_R^2}{4} + t_j \tau_R \right) \sin^2 \left( \omega t_j + \frac{\omega\tau_R}{2} + \varphi \right) \quad (\text{C7})$$

$$\approx \tau_R^2 \xi^2 \sin^2 \varphi \left[ \frac{\tilde{\tau}^2}{6} (N + 3N^2 + 2N^3) + \frac{\tau_R^2 N}{4} + \frac{\tau_R \tilde{\tau}}{2} (N + N^2) \right] \quad (\text{C8})$$

$$\approx \tau_R^2 \xi^2 \sin^2 \varphi \left[ \frac{\tilde{\tau}^2 N^3}{3} + O(N^2) \dots \right] \approx \frac{\xi^2 \tau_R^2 T^3 \sin^2 \varphi}{3\tilde{\tau}}, \quad (\text{C9})$$

where we keep just the leading order in  $N = T/\tilde{\tau}$ .

We can further simplify the expressions above for the total Fisher information of each parameter by taking a phase average, as we did in Eq. (A3), which reduces each of them by a factor of 2. Then, we can write them in compact form as

$$I_{NR}^k(T) = f_{NR}^k \frac{\tau_R^2 T}{2\tilde{\tau}} \exp(-2\tau_R/T_2^*), \quad (\text{C10})$$

which corresponds to the expression provided on the main text, with  $f_{NR}^1 = \xi^2 T^2 / 3$ ,  $f_{NR}^2 = 1$  and  $f_{NR}^3 = \xi^2$ .

The Fisher information for a dynamical decoupling sequence can be immediately calculated using Eq. (B3). Note that in a dynamical decoupling sequence, the phase  $\varphi$  of the external signal will be random, and the sequence will gather no information about it. This means that in order to fairly compare the information about the frequency and the amplitude gathered on a dynamical decoupling sequence, to that acquired for the same parameters on a correlated Ramsey protocol of equal duration, we need to consider the uncertainty about the phase by again taking the average with respect to it. Then, for a dynamical decoupling sequence of total duration  $T$ , the Fisher information is

$$I_{DD}^1(T) = \frac{\xi^2 T^4}{2\pi^2} \operatorname{sinc}^2 \left( \frac{\delta T}{2} \right) e^{-2T/T_2} \approx f_{DD}^1 \frac{T^2}{2\pi^2} e^{-2T/T_2}, \quad (\text{C11})$$

for the frequency and

$$I_{DD}^2(T) = \frac{2T^2}{\pi^2} \operatorname{sinc}^2 \left( \frac{\delta T}{2} \right) e^{-2T/T_2} \approx f_{DD}^2 \frac{T^2}{2\pi^2} e^{-2T/T_2}, \quad (\text{C12})$$

for the amplitude. Then,  $f_{DD}^1 = 3f_{NR}^1$  while  $f_{DD}^2 = 4f_{NR}^2$ . Note that in both equations we consider the low detuning limit  $\delta \rightarrow 0$ .

#### Appendix D: Approximate gain comparison

In this section, we show that the results for the gain presented on Fig. 2 in the main text, which were calculated exactly, are well reproduced with the approximate formula

$$\lim_{\omega \rightarrow 0} g^k = e^{2\left(\frac{T}{\tau_2} - \frac{\tau_R}{\tau_2^2}\right)} \frac{\pi^2 \tau_R^2}{T \tilde{\tau}} f^k, \quad (\text{D1})$$

with  $f^1 = 1/3$  and  $f^2 = 1/4$ . We can see that the trends observed in the exact results are well captured by the approximate formula Eq. (D1), despite deviations [especially in Fig. 4(b)], that can be attributed to the different approximations considered, specially truncating the number of terms with  $T$  on Eq. (C9), which, as all other approximations taken, favours dynamical decoupling sequences, in spite of which most scenarios of low frequency still show the advantage of performing correlated Ramsey measurements.

The results presented here show that, despite the approximations taken, in the low frequency limit, the approximate formula Eq. (D1) can be used to estimate in a simple way the performance of a given correlated Ramsey protocol as compared to the equivalent dynamical decoupling sequence, allowing to choose the best Ramsey sequence parameters that maximize the gain.

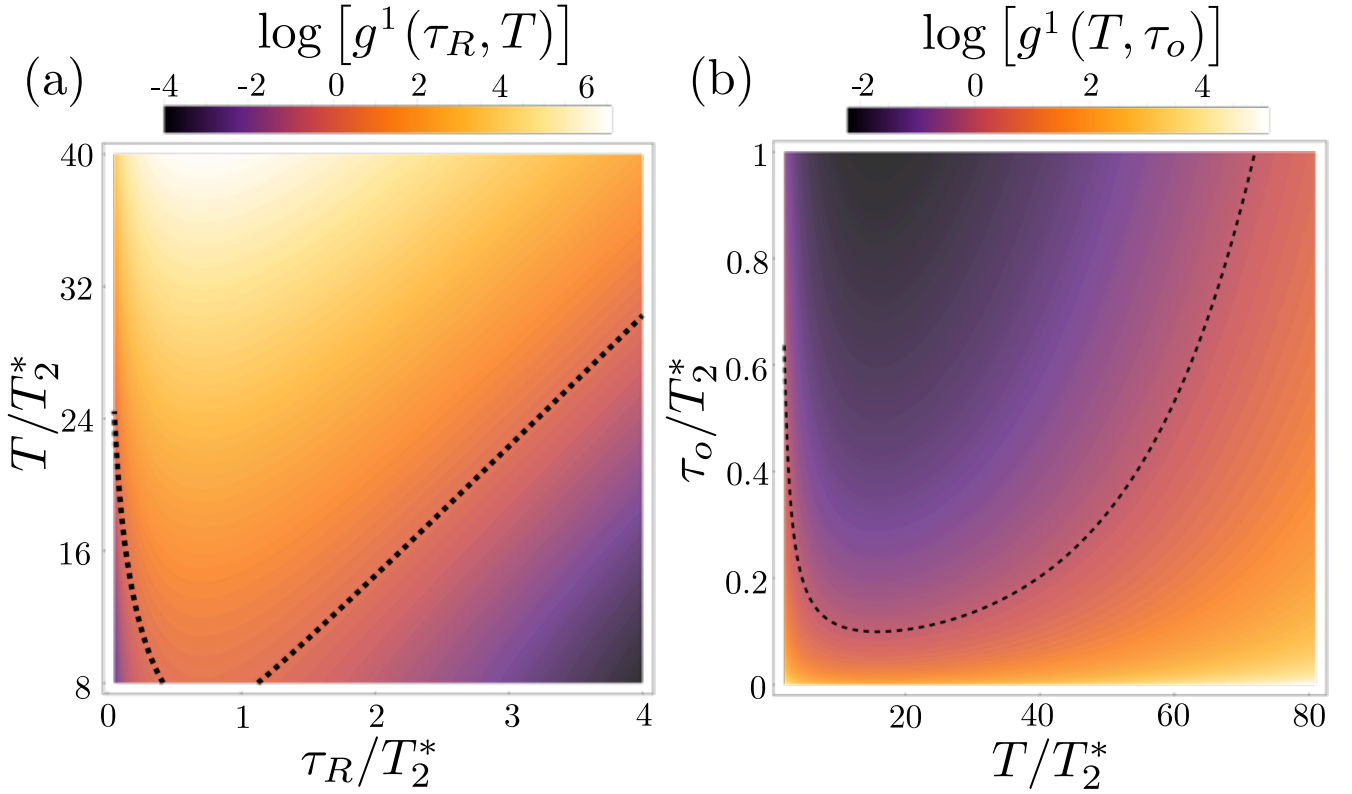


Figure 4. Logarithm of the approximate gain  $g_1$  in Eq. (D1). In (a)  $T_2 = 8T_2^*$  for a dynamical decoupling measurement of eight pulses, with  $\tilde{\tau} = 0.5 + \tau_R$ . (b) For a fixed  $T_2 = 30T_2^*$  in a Hahn echo sequence, the total measurement time  $T$  changes continuously from  $2T_2^*$  to  $40T_2^*$  to detect signals of frequency  $2\pi/T$ . Here  $\tau_R = 0.5T_2^*$  such that  $\tilde{\tau} = 0.5T_2^* + \tau_o$ . In both figures the dashed line shows the boundary  $g^1 = 1$ , and we consider the amplitude  $\xi$  to be the same in both protocols, such that  $g^1$  does not depend on  $\xi$ .